Journal of Membrane Science 322 (2008) 475–483

Contents lists available at ScienceDirect

Journal of Membrane Science

journal homepage: www.elsevier.com/locate/memsci

A combined osmotic pressure and cake filtration model for crossflow nanofiltration of natural organic matter

Supatpong Mattaraj[a,*], Chalor Jarusutthirak[b], Ratana Jiraratananon[c]

[a] Department of Chemical Engineering, Faculty of Engineering, Ubon Ratchathani University, Ubon Ratchathani 34190, Thailand
[b] Department of Chemistry, Faculty of Science, King Mongkut's Institute of Technology Ladkrabang, Bangkok 10520, Thailand
[c] Department of Chemical Engineering, Faculty of Engineering, King Mongkut's University of Technology Thonburi, Bangkok 10140, Thailand

ARTICLE INFO

Article history:
Received 11 April 2008
Received in revised form 21 May 2008
Accepted 26 May 2008
Available online 7 July 2008

Keywords:
Cake filtration
Nanofiltration
Natural organic matter
Osmotic pressure

ABSTRACT

A combined osmotic pressure and cake filtration model for crossflow nanofiltration of natural organic matter (NOM) was developed and successfully used to determine model parameters (i.e. permeability reduction factor (η) and specific cake resistance (α_{cake})) for salt concentrations, NOM concentrations, and ionic strength of salt species (Na^+ and Ca^{++}). In the absence of NOM, with increasing salt concentration from 0.004 to 0.1 M, permeability reduction factor (η)) decreased from 0.99 to 0.72 and 0.94 to 0.44 for monovalent cation (Na^+) and divalent cation (Ca^{++}), respectively. This reduced membrane permeability was due to salt concentrations and salt species. In the presence of NOM, specific cake resistance tended to increase with increasing NOM concentration and ionic strength in the range of 0.85×10^{15}–3.66×10^{15} m kg^{-1}. Solutions containing divalent cation exhibited higher normalized flux decline (J_v/J_{vo} = 0.685–0.632) and specific cake resistance ($\alpha_{cake} = 2.89 \times 10^{15}$–$6.24 \times 10^{15}$ m kg^{-1}) than those containing monovalent cation, indicating a highly compacted NOM accumulation, thus increased permeate flow resistance during NF filtration experiments. After membrane cleaning, divalent cation exhibited lower water flux recovery than monovalent cation, suggesting higher non-recoverable ($R_{non\text{-}rec}$) resistance than monovalent cation.

1. Introduction

Nanofiltration (NF) is widely increasing in the application of drinking water treatment due to high removal efficiency in natural organic matter (NOM), the disinfection by-product (DBP) precursors during chlorination process, and in water softening for removing divalent cations from natural waters [1]. Nanofiltration membranes have molecular weight cut-offs (MWCO) ranging between 300 and 1000 Da [2], while the performances of NF membranes lie between reverse osmosis (RO) membranes (high operating pressure from 1400 to 6800 kPa) and ultrafiltration (UF) membranes (low operating pressure from <70 to 500 kPa) [3]. The separation mechanism of NF membranes is described in terms of charge and sieving effect [4]. Sieving effect is related to solute size responsible for the rejection of uncharged solutes by NF membranes, while charge effect is influenced by the electrostatic interactions between the ion species/valence types and membrane charges, as explained by the Donnan exclusion phenomena [5].

Natural organic matter is considered as a major cause of membrane fouling during NF [6]. NOM components consist of a heterogeneous mixture of complex organic materials, including humic substances, low molecular weight (hydrophilic) acids, proteins, carbohydrates, carboxylic acids, amino acids, and hydrocarbons [7]. Humic substances, the predominant compounds of NOM in surface waters, are amorphous, acidic, yellow-to-brown in color, hydrophilic, and chemically complex polyelectrolytes with the molecular weights ranging from a few hundreds to tens of thousands [8]. They comprise a large fraction of the dissolved organic matter (DOM), typically 30–80% of dissolved organic carbon (DOC) [9]. Molecular weight ranges of aquatic humic substances are from 500 to 5000 [10]. The major functional groups include carboxylic acids, phenolic hydroxyl, carbonyl, and hydroxyl groups [9].

Solution chemistry (i.e. ionic strength, mono- and divalent cations) can influence membrane performance (i.e. solution flux decline and rejection [11]). Increased ionic strength can increase solution flux decline, while divalent cation has a greater flux decline than monovalent cation in membrane fouling [12]. Concentration of salt solutions by NF membranes can result in enhanced rejections depending on ion species [13]. Divalent cations have significant effects on membrane surface charge [14], thus affecting membrane performance. The rejections of divalent cation (calcium) and

* Corresponding author. Tel.: +66 45 353 344; fax: +66 45 353 333.
E-mail addresses: mattas@ubu.ac.th, supatpong.m@hotmail.com (S. Mattaraj), kjchalor@kmitl.ac.th (C. Jarusutthirak), ratana.jir@kmutt.ac.th (R. Jiraratananon).

0376-7388/$ – see front matter © 2008 Elsevier B.V. All rights reserved.
doi:10.1016/j.memsci.2008.05.049

monovalent cation (sodium) were reported to range approximately 13–96% and 10–87%, respectively [15].

In our previous work [16], we investigated different factors affecting crossflow nanofiltration performances in natural organic matter rejection and flux decline. Four mathematical models (i.e. pore blocking, pore constriction, intermediate, and cake formation) were used to interpret membrane performances of NF membrane. However, we could not apply those mathematical models for solutions having salt alone. This was possibly affected by osmotic pressure caused by high salt concentration at the membrane surface. In addition, solutions having NOM were significantly affected by cake formation, especially at high NOM concentration and ionic strength, while model parameters were not characterized for specific cake resistance. Therefore, this paper integrates mathematical models for osmotic pressure caused by salt solution and cake filtration model obtained from NOM solution during crossflow nanofiltration. The objective of this study was to determine model parameters, i.e. permeability reduction factor (η) based on osmotic pressure effect and specific cake resistance (α_{cake}) using a combined osmotic pressure and cake filtration model. The results of this work could provide an evidence for changes in the model parameters as a function of salt concentrations, NOM concentrations, and ionic strength of salt species (sodium and calcium). The model parameters corresponded to the combination effects of osmotic pressure by salts/ion species that changed membrane permeability and cake formation caused by NOM accumulation at the membrane surface. The model parameters could give an insight interpretation of flux decline and rejection characteristics during crossflow NF of NOM with the presence of salts. The effects of ion species/valence types were investigated to compare solution flux curves with different solution chemistry.

2. Theory

2.1. Mass balance

The overall system mass balance model can be determined based on the bench-scale crossflow NF test cell with a recycle loop [16]. It is described as a completely stirred tank reactor (CSTR). The mass balance can be written as follows:

$$V_{sys}\frac{dC_{reten}}{dt} = Q_{feed}C_{feed} - Q_{reten}C_{reten} - Q_{perm}C_{perm} - k_a(C_{ss} - C_{reten}) \times V_{sys} \quad (1)$$

where V_{sys} is the system volume (about 72 mL); Q and C are the subscriptions for flow and concentration in the feed line (feed), in the retentate line (reten), and in the permeate line (perm); C_{ss} is the steady-state concentration in the retentate line; k_a is the overall mass transfer coefficient (min^{-1}) ($=k_1a_s$); k_1 is the mass transfer coefficient ($m\,s^{-1}$) equaling to the ratio between salt diffusion coefficient (D) and boundary layer thickness (δ); a_s is the volumetric specific surface area ($m^2\,m^{-3}$) that equals to the ratio between the effective membrane surface area and the system volume; t is the operating time (min). The units of flow and concentration are $mL\,min^{-1}$ and $mg\,L^{-1}$ or $mol\,L^{-1}$, respectively, depending on solution types. Using a fourth-order Runge–Kutta routine, the overall mass transfer coefficient and the steady-state concentration were varied to minimize the sum of squared error (SSE) for each feed solution.

2.2. Solution flux

Solution flux can be determined as a function of membrane permeability, L_p ($LMH\,kPa^{-1}$), and the net transmembrane pressure gradient ($\Delta P - \sigma\Delta\pi$) (kPa), while the non-recoverable fouling occurs in many instances during filtration, imparting an additional resistance to solution flux [3]:

$$J_v = L_p(\Delta P - \sigma\Delta\pi) = \frac{(\Delta P - \sigma\Delta\pi)}{\mu(R_m + R_{non\text{-}rec})} \quad (2)$$

where J_v is the solution flux ($L\,m^{-2}\,h^{-1}$, LMH); ΔP is the averaged transmembrane pressure (kPa); σ is the osmotic reflection coefficient (estimated by the intrinsic membrane rejection, $R_{mem} = 1 - C_{perm}/C_{mem}$); C_{mem} is the concentration at the membrane surface; $\Delta\pi$ is the difference in osmotic pressure of the solution at the membrane and in permeate line, $\Delta\pi = \pi_{mem} - \pi_{perm}$ (kPa); R_m is the membrane hydraulic resistance (m^{-1}); and $R_{non\text{-}rec}$ is the non-recoverable resistance occurring during filtration (m^{-1}); and μ is the dynamic viscosity ($kg\,m^{-1}\,s^{-1}$).

Under constant-pressure operation, and assuming constant membrane permeability and in the absence of NOM cake on membrane surface, the change in solution flux is related to the change in osmotic pressure as a result of solute accumulation at the membrane surface:

$$\frac{dJ_v}{dt} = -\frac{\sigma}{\mu(R_m + R_{non\text{-}rec})}\frac{d\Delta\pi}{dt} \quad (3)$$

The osmotic pressure is directly related to salt concentration, with π (kPa) $= \alpha C$ ($mol\,L^{-1}$), where $\alpha = 4814.5$ (NaCl) [3] and $\alpha = 7418.8$ ($CaCl_2$) at 25 °C (calculated using Van't Hoff equation). The permeate concentration is correlated to the concentration at the membrane surface by the rejection, $C_{perm} = (1 - R_{mem})C_{mem}$. Making these substitutions,

$$\frac{dJ_v}{dt} = -\frac{\sigma\alpha}{\mu(R_m + R_{non\text{-}rec})}\left(\frac{dC_{mem}}{dt} - \frac{dC_{perm}}{dt}\right) = -\frac{\sigma\alpha R_{mem}}{\mu(R_m + R_{non\text{-}rec})}\left(\frac{dC_{mem}}{dt}\right) \quad (4)$$

The interface concentration (C_{mem}) is calculated from $\sigma\Delta\pi = \sigma(\pi_{mem} - \pi_{perm})$ under steady-state condition. The value of σ is assumed to be equal to the intrinsic rejection for each salt concentration. From the experiments, the ratio $\beta = C_{mem}/C_{reten}$ (salt concentration polarization) is related to salt concentration. Taking this parameter in the above equation and having an additional term of permeability reduction factor due to the effect of salt (η), the change in solution flux with time can be rewritten as follows:

$$\frac{dJ_v}{dt} = -\eta\frac{\sigma\alpha R_{mem}\beta}{\mu(R_m + R_{non\text{-}rec})}\left(\frac{dC_{reten}}{dt}\right) \quad (5)$$

where $\eta(1/\mu(R_m + R_{non\text{-}rec})) = \eta L_p = L_{p,s} = (1/\mu(R_{m,s} + R_{non\text{-}rec}))$ ($L_{p,s}$ is the membrane permeability in the presence of salt solution). The membrane resistance in the presence of salt ($R_{m,s}$) including the permeability reduction factor can be determined as follows:

$$R_{m,s} = \frac{R_m + (1 - \eta)R_{non\text{-}rec}}{\eta} \quad (6)$$

In Eq. (5), the change in the retentate concentration with time can be calculated from the mass balance as described in Eq. (1).

2.3. Combined osmotic pressure and cake filtration model

A combined osmotic pressure and cake filtration model can be developed to describe the nanofiltration performance of a solution containing both salt and NOM. From the previous work, the fouling of nanofiltration membranes can be described by cake filtration model [17,18]. The model has also been used to describe flux in

ultrafiltration and microfiltration [19,20]. The cake filtration model incorporates an additional term of cake resistance (R_c) as follows:

$$J_v = \frac{(\Delta P - \sigma\Delta\pi)}{\mu(R_{m,s} + R_{non\text{-}rec} + R_c)} \quad (7)$$

In our work, we describe the combination effects of osmotic pressure and cake with the change in solution flux as a function of time. The change in solution flux is related to the change in osmotic pressure as a result of salt concentration polarization, and the change in the hydraulic resistance of the NOM cake formed on the membrane surface:

$$\frac{dJ_v}{dt} = -\frac{\sigma_s\alpha_s R_{mem,s}\beta_s}{\mu(R_{m,s} + R_{non\text{-}rec} + R_c)}\left(\frac{dC_{reten,s}}{dt}\right) - \frac{J_v}{(R_{m,s} + R_{non\text{-}rec} + R_c)}\left(\frac{dR_c}{dt}\right) \quad (8)$$

Therefore, Eq. (8) is the combined osmotic pressure and cake filtration model for crossflow nanofiltration. The subscript s refers to salt species (i.e. NaCl or $CaCl_2$). In the results, normalized solution flux (J_v/J_{vo}) is determined by the ratio between solution flux (J_v) and an initial solution flux (J_{vo}). In the cake filtration with constant specific cake resistance (α_{cake}), the change in cake resistance is related to the rate of change in cake mass, m_{cake} (kg), which equals to the net rate of mass transport towards the membrane surface, i.e., the convective flux, J_v, minus the effective flux, J^* (LMH), associated with back-transport resulting from crossflow. Therefore,

$$\frac{dR_c}{dt} = \alpha_{cake}\frac{dm_{cake}}{A_m dt} = \alpha_{cake}C_{reten,NOM}(t)(J_v - J^*) \quad (9)$$

where α_{cake} is the specific cake resistance ($m\,kg^{-1}$), $C_{reten,NOM}$ is the NOM concentration in the retentate line ($kg\,m^{-3}$) and A_m is the membrane area (m^2). The specific cake resistance, as predicted by the Carman–Kozeny equation, can be determined as a function of cake porosity (ε_{cake}) (–), density (ρ) ($kg\,m^{-3}$), particle diameter (d_p) (m) as follows [21]:

$$\alpha_{cake} = \left(\frac{180(1-\varepsilon_{cake})^2}{\rho d_p^2 \varepsilon_{cake}^3}\right) \quad (10)$$

Eqs. (8) and (9) can be determined using the fitting parameters (i.e. specific cake resistance and the effective back-transport flux) in a fourth-order Runge–Kutta routine in order to minimize the sum squared errors between the experimental data and estimated data from cake filtration model. In this work, the combined osmotic pressure and cake filtration model (Eq. (8)) was applied with the experimental results in order to determine model parameters with different solution conditions.

3. Experimental

3.1. Natural organic matter (NOM) and Isolation

Natural organic matter, obtained from the surface water reservoir at Ubon Ratchathani's University (UBU), Thailand, was isolated by using a polyamide thin-film composite (TFC) reverse osmosis membrane (model: AG4040F-spiral wound crossflow, GE osmonics, USA). The isolation procedure was previously described by Jarusutthirak et al. [16] and by Kilduff et al. [22]. Natural water characteristics were previously shown by Jarusutthirak et al. [16]. The feed solutions for NF experiments were prepared by mixing NOM isolates and/or salts with deionized water to obtain the required concentrations.

3.2. Crossflow nanofiltration experiments

Crossflow nanofiltration experiments were carried out by using a bench-scale crossflow nanofiltration test cell with a recycle loop [12,16]. The system volume (V_{sys}) was approximately 72 mL. This was obtained by a tracer study characterized with the dispersion and tanks-in-series model as described by Levenspiel [23]. Thin-film nanofiltration membrane, obtained from GE Osmonics, Inc., USA, was used to investigate flux decline and rejection characteristics during NF experiments. The membrane information and filtration procedure was previously reported by Jarusutthirak et al. [16]. Membrane sheets were cleaned and pre-compacted with initial water flux of 45 LMH. After membrane compaction, average membrane permeability (L_p) was approximately $4.152 \times 10^{-8} \pm 0.062 \times 10^{-8}\ m\,s^{-1}\,kPa^{-1}$ ($0.149\ LMH\,kPa^{-1}$, number of samples are 16 samples) (95% confidence interval) at 25 °C. The membrane hydraulic resistance ($R_m = 1/\mu L_p$) was also determined to be $2.694 \times 10^{13}\ m^{-1}$ (at 25 °C). The nanofiltration sheets were stored in 1% $Na_2S_2O_5$ and kept in a refrigerator (4 °C) to minimize bacterial activity.

3.3. Analytical methods

NOM concentrations were measured as dissolved organic matter using total organic carbon analyzer (Shimadzu corporation, TOC-VCPH model, Japan). Standard solutions were prepared using potassium hydrogen phthalate in deionized water, which was used as a blank. UV absorbance was measured using a UV–vis spectrophotometer (Shimadzu corporation, model UV mini 1240, Japan). Conductivity and solution pH were measured using conductivity meter (model: inoLab cond Level 2, Germany) and pH meter (model: inoLab pH level 1, Wissenschaftlich-Technische Werkstatten, GMBH, Germany), respectively. Ionic strength of samples was calculated using a correlation between conductivity and ionic strength; for NaCl standards, I.S. ($mol\,L^{-1}$) = $0.5\Sigma C_i Z_i^2 = 9.5 \times 10^{-6}$ ($\mu S\,cm^{-1}$) and for $CaCl_2$ standard, I.S. ($mol\,L^{-1}$) = 1.429×10^{-5} ($\mu S\,cm^{-1}$).

3.4. Membrane cleaning

After filtration was terminated, two steps of cleaning, i.e. hydrodynamic cleaning followed by chemical cleaning, were performed: first, for hydrodynamic cleaning, DI water was recirculated in the recycle loop for 30 min with a crossflow velocity of 0.25 m/s, which was higher than that during filtration operation. For chemical cleaning, alkaline solution (using NaOH) with pH of 10 was first used to recirculate in the system, and followed with acidic solution (using HCl) with pH of 3 at a crossflow velocity of 0.25 m/s for 30 min each. After each cleaning, water fluxes with different operating pressures were measured to determine water flux recovery.

4. Results and discussion

4.1. Effect of NaCl concentration on normalized solution flux and model parameter

Fig. 1 illustrates the effect of NaCl concentration on normalized solution flux. Dot points were the experimental data, while the solid lines were the values obtained from the mathematical model (Eq. (5)). Normalized solution flux curve decreased with increasing NaCl concentration. The reason for a flux decline was an increase of the osmotic pressure of the retentate as its concentration was increased due to a continuous removal of the

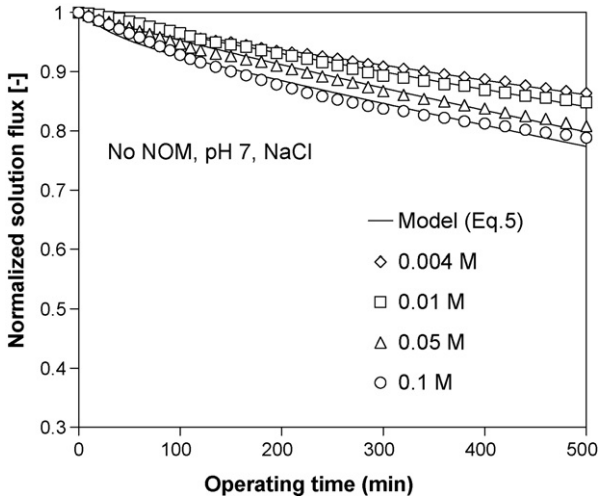

Fig. 1. Effect of NaCl concentration on normalized solution flux.

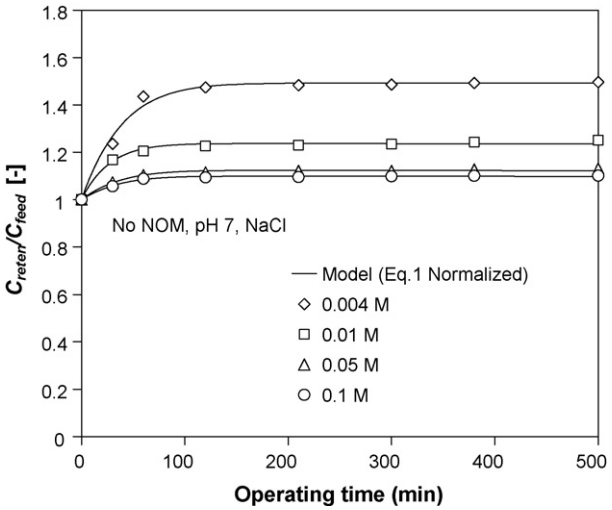

Fig. 2. Normalized retentate salt concentrations during NF operation.

permeate. Permeability reduction factor (η) was the model parameter fitted to the experimental data (based on Eq. (5)). Table 1 shows model parameters and nanofiltration performance at different initial salt concentrations. In the absence of NOM and pH of 7, increased NaCl concentrations from 0.004 to 0.1 M reduced normalized flux and permeability reduction factor from 0.864 to 0.788 and 0.99 to 0.72, respectively. This was possibly caused by the increased osmotic pressure as mentioned earlier. Fig. 2 exhibits normalized retentate salt concentrations in a recycle loop with different initial salt concentrations. The solid lines shown in the figure were determined using the mass balance (Eq. (1)). The lines were the ratio between retentate salt concentrations and feed salt concentrations. It was observed that normalized retentate salt concentrations decreased with increasing feed salt concentrations, possibly caused by the effect of salt rejection. Increased salt concentrations from 0.004 to 0.1 M tended to decrease the retentate salt rejections from 35.8% to 10% along with filtration period (see Table 1). The results suggested that the effect of ions at the membrane–solution interface enhanced a reduction of electrical double layer thickness, thus allowing salt passage through the membrane surface. Negatively charged chloride ion was possibly repelled from the negatively charged membrane, while positively charged sodium ion was attracted to the membrane surface, indicating increased ion concentration in the membrane matrix and increased screening of charge moieties [24]. This can enhance the changes in the membrane pore size due to polymer matrix compaction. This corresponded to reduced permeability reduction factor (decreased membrane permeability). With increasing salt concentration from 0.004 to 0.1 M, the intrinsic membrane rejection decreased from 44.2% to 18%, while the salt concentration polarization (β) decreased from 1.149 to 1.097. Similar trends were observed with the results from Fig. 2. The ratios of J_v/k_1 were relatively constant about 0.318–0.3. The permeability reduction factors (η) decreased from 0.99 to 0.72, indicating higher values than those of tight polyamide NF-70 membrane, previously studied by Kilduff et al. [3]. They reported that the permeability reduction factors (η) decreased from 0.96 to 0.52 with increasing salt concentration from 0.004 to 0.1 M NaCl. In addition, the averaged mass transfer coefficient of 3.39×10^{-5} m s^{-1} showed a higher value than that of the tight polyamide NF-70 membrane (1.6×10^{-5} m s^{-1}) determined using the same mass balance (Eq. (1)). This indicated less boundary layer thickness (δ) of salt solution for the loose NF membrane than that for the tight NF membrane. For the tight NF membrane, the intrinsic membrane rejection showed higher values than those of the loose NF membrane. The rejections decreased from 90% to 72.5% with increasing salt concentration from 0.004 to 0.1 M NaCl.

Table 1
Model parameters and nanofiltration performance at different salt concentrations

Parameters	NaCl concentration (M)			
	0.004	0.01	0.05	0.1
J_v/J_{vo} (–)	0.864	0.848	0.808	0.788
$J_v \times 10^6$ (m s^{-1})	10.8	10.6	10.1	9.85
C_{mem} (M)	0.0077	0.0162	0.0653	0.1216
C_{reten} (M)	0.0067	0.0143	0.0589	0.1108
C_{perm} (M)	0.0043	0.0112	0.0513	0.0997
β (C_{mem}/C_{reten})	1.149	1.133	1.109	1.097
R_{feed} (%)	5.6–18.0 (6.9)	2.2–5.8 (3.5)	1.4–5.9 (3.7)	0.1–3.0 (1.6)
R_{reten} (%)	33.6–38.0 (35.8)	19.3–22.0 (21.4)	12.3–14.4 (12.9)	8.1–10.6 (10.0)
R_{mem} (%)	44.2	30.9	21.4	18.0
η	0.99	0.94	0.78	0.72
ηL_p (m s^{-1} kPa^{-1}) $\times 10^8$	4.11	3.92	3.24	2.98
k_1 (m s^{-1}) $\times 10^5$	3.60	3.36	3.32	3.28
J_v/k_1	0.318	0.315	0.304	0.30
Average k_1 (m s^{-1})	3.39×10^{-5}			

Operating conditions: initial flux = 1.25×10^{-5} m s^{-1}, crossflow velocity = 0.1 m s^{-1}, recovery = 0.85, temperature = 25 °C. Average membrane permeability (L_p) was $4.152 \times 10^{-8} \pm 0.062 \times 10^{-8}$ m s^{-1} kPa^{-1} (0.149 LMH kPa^{-1}). The values in the parenthesis are the averaged rejections.

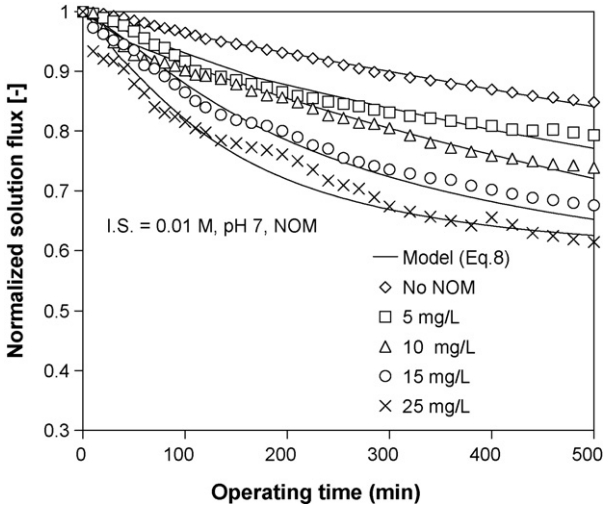

Fig. 3. Effect of NOM concentration on normalized solution flux.

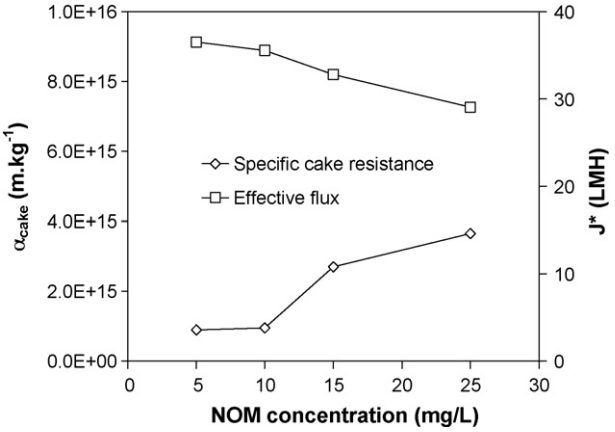

Fig. 4. Effect of NOM concentration on specific cake resistance and effective flux.

4.2. Effect of NOM concentration on normalized solution flux and model parameter

Fig. 3 shows the effect of NOM concentration on normalized solution flux. Dot points were the experimental data, while the solid lines were followed with the combined osmotic pressure and cake filtration model (Eq. (8)). NOM concentration ranged from 0 to 25 mg L^{-1} with ionic strength of 0.01 M NaCl and solution pH of 7. Model parameters and nanofiltration performance on the influence of NOM concentration are tabulated in Table 2. In the absence of NOM, normalized solution flux decreased based on the effect of osmotic pressure caused by increased salt concentration at the membrane surface. At the ionic strength of 0.01 M and pH of 7, normalized solution flux and retentate salt rejection were approximately 0.848 and 21.4%, respectively. In the presence of NOM, normalized solution flux tended to decrease from 0.793 to 0.614 with increasing NOM concentration from 5 to 25 mg L^{-1}, while the retentate salt rejection slightly increased from 25.3% to 28.2%. In the similar trend, increased NOM concentration from 5 to 25 mg L^{-1} increased the feed and retentate NOM rejections from 75.3% to 88.4% and 94.3% to 97.1%, respectively. Solutions having high NOM concentration of 25 mg L^{-1} resulted in the highest rejection of salt and NOM rejection in the feed and retentate line, possibly due to combination effects of osmotic pressure by salt concentration and cake formation by NOM accumulation. The experimental results suggest the reduction of charge repulsion due to charge interaction between negatively charged NOM and positively charged sodium ion, causing NOM cake formation at the membrane surface. In addition, the negatively charged NOM molecules can be repelled from the membrane surface, indicating an increase in the averaged feed and retentate rejections of NOM. With the constant membrane resistance in the presence of salt ($R_{m,s}$), the fitted parameters (i.e. the specific cake resistance, α_{cake} and the effective flux, J^*), can be obtained using the combined osmotic pressure and cake filtration model (Eq. (8)). From the table, increased NOM concentration ranging from 5 to 25 mg L^{-1} increased specific cake resistance from 0.89×10^{15} to 3.66×10^{15} m kg^{-1} (increased by 75.7%), while the effective flux tended to decrease with increasing NOM concentration as shown in Fig. 4. The increase in specific cake resistance can be explained by a decrease in cake porosity with increasing NOM concentration, causing more compacted NOM accumulation at the membrane surface. This could be explained using Eq. (10). The specific cake resistance can be sensitive to changes in solution properties. The membrane used in this study resulted in lower specific cake resistance and flux decline than that of the tight polyamide NF-70 membrane [3]. This suggests that membrane properties have significant effects on changes in solution flux due to the combination effects of osmotic pressure by salt concentration and NOM cake formation at the membrane surface.

4.3. Effect of ionic strength on normalized solution flux in the presence of NOM

Solutions having constant 10 mg L^{-1} NOM and pH of 7 were investigated at different ionic strengths. Fig. 5 shows the effect of ionic strength on normalized solution flux. Dot points were the experimental data while the solid lines were fitted well with the combined osmotic pressure and cake filtration model (Eq. (8)). Model parameters and nanofiltration performance on the effect of ionic strength are tabulated in Table 3. With increasing ionic strength from 0.004 to 0.1 M NaCl, normalized solution flux decreased from 0.763 to 0.69. The increase in ionic strength

Table 2
Model parameters and nanofiltration performance: effect of NOM concentration

Parameters	NOM concentration (mg L^{-1})			
	5	10	15	25
J_v/J_{vo} (–)	0.793	0.739	0.676	0.614
$J_v \times 10^6$ (m s^{-1})	9.9	9.2	8.5	7.7
$R_{feed,s}$ (%)	3.6–5.2 (4.3)	4.2–9.1 (5.4)	2.7–12.2 (4.6)	4.2–11.6 (5.7)
$R_{reten,s}$ (%)	24.6–27.0 (26.3)	24.3–26.5 (25.3)	22.9–27.6 (25.4)	23.5–30.5 (28.2)
$R_{feed,NOM}$ (%)	74.4–77.3 (75.3)	76.4–81.0 (78.5)	75.1–83.9 (77.7)	87.0–91.1 (88.4)
$R_{reten,NOM}$ (%)	92.5–94.9 (94.3)	92.7–95.8 (94.9)	93.3–95.9 (95.0)	96.0–97.6 (97.1)
α_{cake} (m kg^{-1}) $\times 10^{-15}$	0.89	0.95	2.70	3.66
$J^* \times 10^6$ (m s^{-1})	10.1	9.9	9.1	8.1

The values in the parenthesis are the averaged rejections.

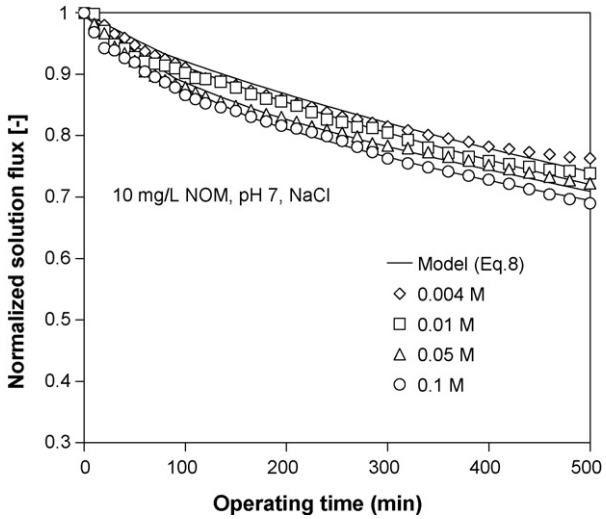

Fig. 5. Effect of ionic strength on normalized solution flux.

decreased the salt rejection, indicating charge screening at the membrane surface, thus increased salt passage through the membrane. The feed and retentate salt rejections decreased from 9.6% to 1.7% and from 28.4% to 11.2%, respectively. Braghetta et al. [24] explained that increased ionic strength would normalize charge at the membrane surface (sulfonated polysulfone NF membrane) and compressed a double layer thickness (i.e. membrane compaction occurred). Solutions having NOM showed higher salt rejection than those having no NOM, especially at high ionic strength. This was caused by reduced charge repulsion between positively charged Na^+ and negatively charged NOM. The NOM rejections in the feed ($R_{feed,NOM}$) and retentate line ($R_{reten,NOM}$) reduced from 78.5% to 64.7% and 95.3% to 91.3% with increasing ionic strengths. This suggests the changes in NOM configuration due to reduced charge repulsion between ionized functional groups on NOM molecules. Previous study suggested that NOM molecules are configured more as rigid, compact, and spherocolloidal macromolecules (small hydrodynamic radius) at low pH and high ionic strength or high NOM concentration [25]. This can enhance the passage of the spherocolloidal NOM molecules through the membrane surface, thus decreased NOM rejection. Based on the combined osmotic pressure and cake filtration model, the specific cake resistance increased from 0.85×10^{15} to 2.73×10^{15} m kg^{-1} (increased by about 69%) with increasing ionic strengths from 0.004 to 0.1 M NaCl. The experimental results were possibly explained by reduced charge repulsion between NOM molecules, resulting in more densely compacted NOM layer, thus decreased cake porosity at the membrane surface.

4.4. Effect of divalent cations on normalized solution flux in the presence of NOM

Divalent cation (i.e. Ca^{++}) can significantly influence membrane fouling on NF membrane [1,11]. Fig. 6 shows the effect of divalent cation on normalized solution flux. Solid lines are model fitted to the experimental data, represented as dot points. Model parameters and nanofiltration performance due to the effect of divalent cation are tabulated in Table 4. Solutions containing 10 mg L^{-1} NOM and pH of 7 were tested with different ionic strengths using calcium chloride. It was observed that increased ionic strengths from 0.004 to 0.1 M $CaCl_2$ decreased normalized solution flux from 0.685 to 0.632 (at 8-h operation). The salt rejections increased with increasing ionic strengths using calcium chloride. The averaged salt rejections in the feed and retentate line were about 4.7–11.3% and 24.2–37.9%, respectively. These showed higher salt rejections than those of NaCl solution, indicating calcium–NOM accumulation on the membrane surface. The permeability reduc-

Table 3
Model parameters and nanofiltration performance: effect of ionic strength

Parameters	Ionic strength (M)			
	0.004	0.01	0.05	0.1
J_v/J_{vo} (–)	0.763	0.739	0.723	0.69
$J_v \times 10^6$ (m s^{-1})	9.5	9.2	9.0	8.6
$R_{feed,s}$ (%)	7.1–19.2 (9.6)	4.2–9.1 (5.4)	0.6–8.7 (2.7)	0.1–10.0 (1.7)
$R_{reten,s}$ (%)	27.0–31.9 (28.4)	24.3–26.5 (25.3)	12.1–15.9 (13.7)	10.2–15.9 (11.2)
$R_{feed,NOM}$ (%)	75.9–82.1 (78.0)	76.4–81.0 (78.5)	76.3–81.3 (77.9)	61.6–72.5 (64.7)
$R_{reten,NOM}$ (%)	93.4–96.0 (95.2)	92.7–95.8 (94.9)	92.3–96.4 (95.3)	89.5–92.2 (91.3)
α_{cake} (m kg^{-1}) $\times 10^{-15}$	0.85	0.95	1.53	2.73
$J^* \times 10^6$ (m s^{-1})	9.93	9.9	9.4	8.99

The values in the parenthesis are the averaged rejections.

Table 4
Model parameters and nanofiltration performance: effect of divalent cation

Parameter	$CaCl_2$ concentration (M)			
	0.004	0.01	0.05	0.1
J_v/J_{vo} (–)	0.685	0.664	0.648	0.632
$J_v \times 10^6$ (m s^{-1})	8.56	8.30	8.10	7.90
$R_{feed,s}$ (%)	1.5–13.8 (5.2)	2.3–9.2 (4.7)	7.3–20.6 (11.3)	7.9–22.0 (9.9)
$R_{reten,s}$ (%)	21.4–31.8 (30.9)	23.2–26.2 (24.2)	37.9–38.5 (37.9)	35.3–39.6 (37.8)
β (C_{mem}/C_{reten})	1.272	1.217	1.049	1.036
$R_{feed,NOM}$ (%)	66.4–78.3 (69.9)	79.5–84.7 (82.3)	80.9–84.0 (82.0)	75.7–79.9 (77.3)
$R_{reten,NOM}$ (%)	91.1–96.2 (94.4)	95.1–97.7 (97.0)	93.4–96.6 (95.7)	90.6–96.1 (94.4)
η	0.94	0.76	0.61	0.44
ηL_p (m s^{-1} kPa^{-1}) $\times 10^8$	3.90	3.16	2.53	1.83
α_{cake} (m kg^{-1}) $\times 10^{-15}$	2.89	3.52	5.14	6.24
$J^* \times 10^6$ (m s^{-1})	9.12	9.02	8.86	8.57

The values in the parenthesis are the averaged rejections.

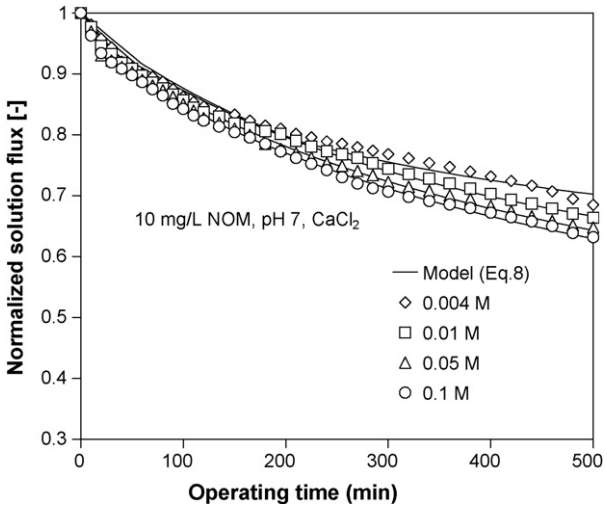

Fig. 6. Effect of divalent cation on normalized solution flux.

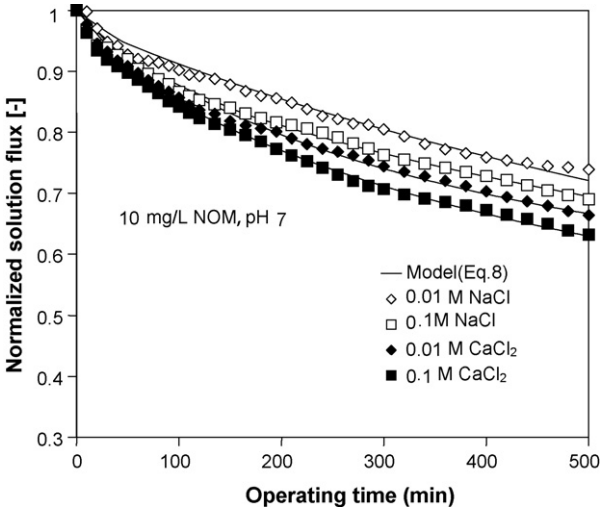

Fig. 7. Effect of mono- and divalent cations on normalized solution flux.

tion factor (η) decreased from 0.94 to 0.44 with increasing ionic strengths. This was possibly caused by reduced charge repulsion between positively charged Ca^{++} ion and negatively charged NF membrane, thus compressing a double layer thickness at the membrane surface. Previous study found that divalent cation caused a marked effect on membrane surface charge [14]. With increasing ionic strengths, averaged NOM rejections in the feed and retentate increased from 69.9% to 82.3% and 94.4% to 97%, respectively. This showed the opposite trend with increasing ionic strengths using monovalent (Na^+) ion, where a change in NOM configuration could dominate the rejection results. The rejections obtained from the divalent cation illustrated relatively high rejections compared with monovalent (Na^+) ion. This resulted in the opposite effect from monovalent (Na^+) ion. This was possibly caused by the dominant effect from a compacted NOM cake formation by decreased charge repulsion between positively charged Ca^{++} ion and negatively charged NOM molecules, thus enhancing NOM accumulation. This corresponds to high specific cake resistance (α_{cake}) about 2.89×10^{15}–6.24×10^{15} m kg^{-1}, respectively (increased by 53.7%). The increase in specific cake resistance could decrease cake porosity, suggesting a densely packed NOM cake layer at the membrane surface. Schafer et al. [1] confirmed that higher calcium concentration caused severe NF fouling and increased non-recoverable fouling. Previous study explained that calcium act with humic carboxyl functional group, suggesting a reduction of NOM charge and electrostatic repulsion between humic macromolecules [11].

Mono- and divalent cations can influence nanofiltration performance (i.e. solution flux and rejection). The model parameters (i.e. permeability reduction factor and specific cake resistance) can be evaluated with the combined osmotic pressure and cake filtration model (Eq. (8)). This describes the effect of osmotic pressure caused by increased salt concentration polarization, while the effects of cake formation model are based on NOM cake formation at the membrane surface. Fig. 7 exhibits the effect of mono- and divalent cations on normalized solution flux. With similar ionic strengths, solutions having divalent Ca^{++} cation showed greater solution flux decline than those having monovalent Na^+ cation. This suggested that divalent cation had greater effects on charge combination between membrane surface charge and NOM macromolecules than monovalent cation. This could cause higher salt and NOM rejections (previously described). In addition, model parameters could be changed with different ion species. Fig. 8 exhibits the effect of mono- and divalent cations on permeability reduction factor (filled symbols) and specific cake resistance (open symbols). Increased ionic strengths from 0.004 to 0.1 M using mono- and divalent cations tended to decrease the permeability reduction factor and to increase the specific cake resistance. Divalent Ca^{++} cation showed greater values of permeability reduction factor and specific cake resistance than monovalent Na^+ cation. The decreases in permeability reduction factors of mono- and divalent cations were determined to be 0.99–0.72 and 0.94–0.44, respectively. The increases in specific cake resistance of mono- and divalent cations were about 0.85×10^{15}–2.73×10^{15} and 2.89×10^{15}–6.24×10^{15} m kg^{-1}, respectively. The experimental results indicated that divalent cation has a marked effect on reduced charge repulsion between positively charged divalent cation (Ca^{++}) and negatively charged NF membrane, causing a reduced double layer thickness at the membrane surface. This corresponds to lower permeability reduction factor with increasing ionic strengths. Divalent cation influenced an increase in cake formation on the membrane surface. This was caused by a reduction of charge repulsion between NOM molecules by increasing positive calcium ion concentrations. This resulted in an increase in specific cake resistance with increasing ionic strengths.

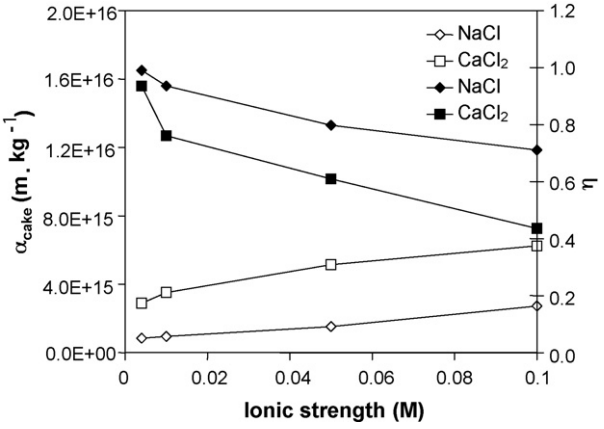

Fig. 8. Effect of mono- and divalent cations on η (filled symbols) and α_{cake} (open symbols).

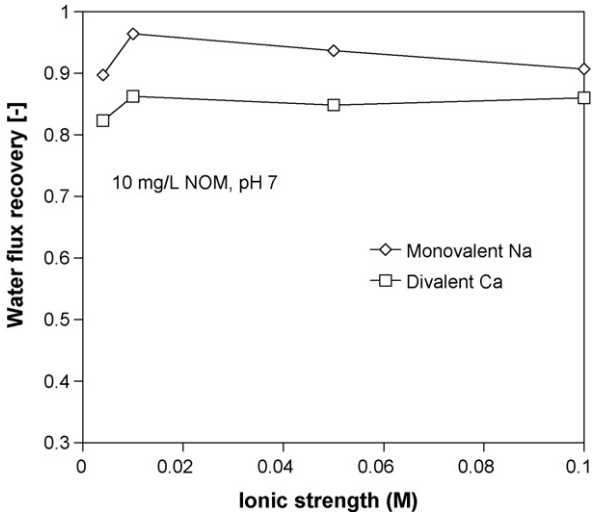

Fig. 9. Water flux recovery after chemical cleaning for mono- and divalent cations.

4.5. Water flux recovery

Fig. 9 describes water flux recovery after chemical cleaning for mono- and divalent cations. The experimental results were taken after hydrodynamic and chemical cleaning of NOM solution. It was observed that water flux recovery was less than 1 for different salt species (Na^+ and Ca^{++}). This suggested different interactions between NOM–salt species and the membrane, causing non-recoverable resistance ($R_{non\text{-}rec}$) on the membrane surface. With increasing ionic strength from 0.004 to 0.1 M, non-recoverable resistances for monovalent Na^+ cation were approximately 2.91×10^{12}, 1.06×10^{12}, 1.85×10^{12}, and 2.58×10^{12}, respectively. For divalent Ca^{++} cation, non-recoverable resistances were about 6.1×10^{12}, 4.52×10^{12}, 4.99×10^{12}, and 4.62×10^{12}, respectively. Divalent Ca^{++} cation resulted in lower water flux recovery (higher $R_{non\text{-}rec}$) than movalent Na^+ cation. This indicated a more compacted Ca–NOM cake layer (lower cake porosity), and thus increased permeate flow resistance during filtration experiments. The experimental results agreed with the results from Wang et al. [26]. They indicated that divalent cations seemed to be more readily adsorbed on the membrane surface than monovalent ions because divalent cations could act as a bridge between the membrane surface and the negatively charged humic acid molecules and also between the negatively charged function groups of humic acid that were not in contact with the membrane, resulting a highly compacted fouling layer at the membrane surface [26].

5. Conclusions

A combined osmotic pressure and cake filtration model for crossflow nanofiltration of NOM solution can be used successfully to characterize model parameters (i.e. permeability reduction factor and specific cake resistance) for salt concentrations, NOM concentrations, ionic strength of salt species (Na^+ and Ca^{++}). This model can be explained in terms of salt and NOM combination, while the mathematical models from the previous work [16] could not be applied to interpret model parameters due to the effect of salt alone and combined salt and NOM solution. Based on the combined osmotic pressure and cake filtration model, permeability reduction factor was used to describe the change in membrane permeability in the presence of salt concentrations and ion species, while specific cake resistance was used to interpret NOM accumulation at the membrane surface. In the absence of NOM, increased NaCl salt concentrations ranging from 0.004 to 0.1 M decreased normalized solution flux, while permeability reduction factor decreased from 0.99 to 0.72. With increasing ionic strengths, divalent cation (Ca^{++}) exhibited greater flux decline than monovalent cation (Na^+), thus corresponding a relatively low permeability reduction factor. This indicated a reduction of charge repulsion between positively charged salt and negatively charged NF membrane, thus decreased double layer thickness at the membrane surface. The results suggested significant effects of charge screening at the membrane surface due to divalent cation. In the presence of NOM, solutions having high NOM concentrations caused a reduction of normalized solution flux, thus resulting in increased specific cake resistances. Solutions having divalent cation presented higher salt rejection and specific cake resistances than those having monovalent cation. This resulted in a reduction of charge repulsion between calcium and NOM functional groups, thus increasing a highly compacted NOM accumulation at the membrane surface (lower cake porosity), thus increased permeate flow resistance during filtration experiments. After membrane cleaning, divalent cation exhibited lower water flux recovery than monovalent cation, suggesting higher non-recoverable ($R_{non\text{-}rec}$) resistance than monovalent cation.

Acknowledgements

The authors would like to thank the Thailand Research Fund (TRF) for TRF senior research scholar grant (no. RTA5080014) and the Commission on Higher Education, Thailand, for financial support. We also would like to thank the Department of Chemical Engineering, Faculty of Engineering, Ubon Rachathani University, Thailand, for all equipments applied in this research.

Nomenclature

a_s	volumetric specific surface area ($m^2\ m^{-3}$)
A_m	membrane area (m^2)
C_{feed}	concentration in the feed line ($mg\ L^{-1}$ or $mol\ L^{-1}$)
C_{mem}	concentration at the membrane surface ($mg\ L^{-1}$ or $mol\ L^{-1}$)
C_{perm}	concentration in the permeate line ($mg\ L^{-1}$ or $mol\ L^{-1}$)
C_{reten}	concentration in the retentate line ($mg\ L^{-1}$ or $mol\ L^{-1}$)
$C_{reten,NOM}$	NOM concentration in the retentate line ($kg\ m^{-3}$)
$C_{reten,s}$	concentration in the retentate line in the presence of salt ($mol\ L^{-1}$)
C_{ss}	steady-state concentration in the retentate line ($mg\ L^{-1}$ or $mol\ L^{-1}$)
d_p	particle diameter (m)
D	salt diffusion coefficient ($m^2\ s^{-1}$)
J^*	effective flux associated with back-transport resulting from crossflow (LMH)
J_v	solution flux ($L\ m^{-2}\ h^{-1}$, LMH)
J_{vo}	initial solution flux ($L\ m^{-2}\ h^{-1}$, LMH)
k_a	overall mass transfer coefficient (min^{-1}) ($=k_1 a_s$)
k_1	mass transfer coefficient ($m\ s^{-1}$)
L_p	membrane permeability ($LMH\ kPa^{-1}$)
$L_{p,s}$	membrane permeability in the presence of salt ($LMH\ kPa^{-1}$)
m_{cake}	cake mass (kg)
P	transmembrane pressure (kPa)
Q_{perm}	flow in the permeate line ($mL\ min^{-1}$)

Q_{reten}	flow in the retentate line (mL min^{-1})
R_c	cake resistance (m^{-1})
R_{feed}	rejection in the feed stream (–)
R_m	membrane hydraulic resistance (m^{-1})
$R_{m,s}$	membrane resistance in the presence of salt (m^{-1})
R_{mem}	intrinsic membrane rejection (–)
$R_{mem,s}$	intrinsic membrane rejection in the presence of salt (–)
$R_{non\text{-}rec}$	non-recoverable resistance (m^{-1})
R_{reten}	rejection in the retentate stream (–)
t	operating time (min)
V_{sys}	system volume (mL)

Greek letters

α	correlation between osmotic pressure and salt concentration (kPa L mol^{-1})
α_{cake}	specific cake resistance (m kg^{-1})
β	salt concentration polarization (–)
δ	boundary layer thickness (m)
ε_{cake}	cake porosity (–)
η	permeability reduction factor (–)
μ	dynamic viscosity (kg m^{-1} s^{-1})
π	osmotic pressure (kPa)
π_{mem}	osmotic pressure at the membrane surface (kPa)
π_{perm}	osmotic pressure in the permeate line (kPa)
ρ	density (kg m^{-3})
σ	osmotic reflection coefficient (–)

References

[1] A.I. Schafer, A.G. Fane, T.D. Waite, Nanofiltration of natural organic matter: removal, fouling and the influence of multivalent ions, Desalination 118 (1998) 109–122.
[2] P. Eriksson, Nanofiltration extends the range of membrane filtration, Environ. Prog. 7 (1) (1998) 58–62.
[3] J.E. Kilduff, S. Mattaraj, G. Belfort, Flux decline during nanofiltration of naturally- occurring dissolved organic matter: effects of osmotic pressure, membrane permeability, and cake formation, J. Membr. Sci. 239 (1) (2004) 39–53.
[4] J. Schaep, B. Van der Bruggen, C. Vandecasteele, D. Wilms, Influence of ion size and charge in nanofiltration, Sep. Pur. Technol. 14 (1998) 155–162.
[5] A. Yaroshchuk, E. Staude, Charged membranes for low pressure reverse osmosis properties and applications, Desalination 86 (1992) 115–134.
[6] A. Seidel, M. Elimelech, Coupling between chemical and physical interaction in natural organic matters (NOM) fouling of nanofiltration membranes: implications for fouling control, J. Membr. Sci. 203 (2002) 245–255.
[7] E. Tipping, Cation binding by humic substances, Cambridge Environmental Chemistry Series, 1948, ISBN 0-521-62146-1.
[8] M. Schnitzer, S.U. Khan, Humic Substances in the Environment, Mercel Decker, New York, 1972.
[9] S.W. Krasner, J.-P. Croue, J. Buffle, E.M. Perdue, Three approaches for characterizing NOM, J. AWWA 88 (6) (1996) 66–79.
[10] E.M. Thurman, Organic Geochemistry of Natural Waters, Martinus Nijhoff/Dr. W. Junk Publishers, Dordrecht, 1985.
[11] S. Hong, M. Elimelech, Chemical and physical aspects of natural organic matter (NOM) fouling of nanofiltration membranes, J. Membr. Sci. 132 (1997) 159–181.
[12] C. Jarusutthirak, S. Mattaraj, R. Jiraratananon, Influence of inorganic scalants and natural organic matter on nanofiltration membrane fouling, J. Membr. Sci. 287 (2007) 138–145.
[13] A. Seidel, J.J. Waypa, M. Elimelech, Role of charge (Donnan) exclusion in removal of Arsenic from water by a negatively charged porous nanofiltration membrane, Environ. Eng. Sci. 18 (2) (2001) 105–113.
[14] A.E. Childress, M. Elimelech, Effect of solution chemistry on the surface charge of polymeric reverse osmosis and nanofiltration membranes, J. Membr. Sci. 119 (1996) 253–268.
[15] A.I. Schafer, A.G. Fane, T.D. Waite, Fouling effects on rejection in the membrane filtration of natural waters, Desalination 131 (2000) 215–224.
[16] C. Jarusutthirak, S. Mattaraj, R. Jiraratananon, Factors affecting nanofiltration performances in natural organic matter rejection and flux decline, Sep. Pur. Technol. 58 (2007) 68–75.
[17] J. Cho, G.L. Amy, J. Pellegrino, Membrane filtration of natural organic matter: initial comparison of rejection and flux decline characteristics with ultrafiltration and nanofiltration membranes, Water Res. 33 (1999) 2517–2526.
[18] J.E. Kilduff, S. Mattaraj, J. Sensibaugh, J.P. Pieracci, Y. Yuan, G. Belfort, Modeling flux decline during nanofiltration of NOM with poly (arylsulfone) nanofiltration membranes modified using UV-assisted graft polymerization, Environ. Eng. Sci. 19 (6) (2002) 477–496.
[19] R.W. Field, D. Wu, J.A. Howell, B.B. Gupta, Critical flux concept for microfiltration fouling, J. Membr. Sci. 100 (1995) 259–272.
[20] L.J. Zeman, A.L. Zydney, Microfiltration and Ultrafiltration: Principles and Applications, M. Dekker, New York, 1996.
[21] M.R. Wiesner, P. Aptel, Mass transport and permeate flux and fouling in pressure-driven processes, in: Water Treatment Membrane Processes, J. Mallevialle, P.E. Odendaal, M.R. Wiesner (Eds.), McGraw-Hill, New York, ISBN 0-07-0019-7-00151996.
[22] J.E. Kilduff, S. Mattaraj, A. Wigton, M. Kitis, T. Karanfil, Effects of reverse osmosis isolation on reactivity of naturally occurring dissolved organic matter in physicochemical processes, Water Res. 38 (4) (2004) 1026–1036.
[23] O. Levenspiel, Chemical Reaction Engineering, third ed., John Wiley & Sons, Inc., 1999.
[24] A. Braghetta, F.A. DiGiano, W.P. Ball, Nanofiltration of natural organic matter: pH and ionic strength effects, J. Environ. Eng., ASCE 123 (7) (1997) 628–641.
[25] K. Ghosh, M. Schnitzer, Macromolecular structures of humic substances, Soil Sci. 129 (5) (1980) 266–276.
[26] Z. Wang, Y. Zhao, J. Wang, S. Wang, Studies on nanofiltration membrane fouling in the treatment of water solutions containing humic acids, Desalination 178 (2005) 171–178.